Effects of atmospheric CO₂ variability of the past 800 kyr on the biomes of southeast Africa

Lydie Dupont, Thibaut Caley, Isla Castañeda

HAL Id: hal-02325008
https://hal.science/hal-02325008

Submitted on 26 Jul 2020

Climate
of the Past

Effects of atmospheric CO_2 variability of the past 800 kyr on the biomes of southeast Africa

Lydie M. Dupont[1], Thibaut Caley[2], and Isla S. Castañeda[3]

[1]MARUM – Center for Marine Environmental Sciences, University of Bremen, Bremen, Germany
[2]EPOC, UMR 5805, CNRS, University of Bordeaux, Pessac, France
[3]University of Massachusetts Amherst, Department of Geosciences, Amherst, MA, USA

Correspondence: Lydie M. Dupont (ldupont@marum.de)

Abstract. Very little is known about the impact of atmospheric carbon dioxide pressure (pCO$_2$) on the shaping of biomes. The development of pCO$_2$ throughout the Brunhes Chron may be considered a natural experiment to elucidate relationships between vegetation and pCO$_2$. While the glacial periods show low to very low values ($\sim$ 220 to $\sim$ 190 ppmv, respectively), the pCO$_2$ levels of the interglacial periods vary from intermediate to relatively high ($\sim$ 250 to more than 270 ppmv, respectively). To study the influence of pCO$_2$ on the Pleistocene development of SE African vegetation, we used the pollen record of a marine core (MD96-2048) retrieved from Delagoa Bight south of the Limpopo River mouth in combination with stable isotopes and geochemical proxies. Applying endmember analysis, four pollen assemblages could be distinguished representing different biomes: heathland, mountain forest, shrubland and woodland. We find that the vegetation of the Limpopo River catchment and the coastal region of southern Mozambique is influenced not only by hydroclimate but also by temperature and atmospheric pCO$_2$. Our results suggest that the extension of mountain forest occurred during those parts of the glacials when pCO$_2$ and temperatures were moderate and that only during the colder periods when atmospheric pCO$_2$ was low (less than 220 ppmv) open ericaceous vegetation including C$_4$ sedges extended. The main development of woodlands in the area took place after the Mid-Brunhes Event ($\sim$ 430 ka) when interglacial pCO$_2$ levels regularly rose over 270 ppmv.

1 Introduction

Understanding the role of atmospheric carbon dioxide pressure (pCO$_2$) is paramount for the interpretation of the of the palaeovegetation record. The effects of low pCO$_2$ on glacial vegetation have been discussed in a number of studies (Ehleringer et al., 1997; Jolly and Haxeltine, 1997; Cowling and Sykes, 1999; Prentice and Harrison, 2009; Prentice et al., 2017) predicting that glacial increases in C$_4$ vegetation favoured by low atmospheric CO$_2$ would have opened the landscape and lowered the tree line. Comparing records of this glacial C$_4$-rich vegetation with modern analogues could have led to estimating more severe aridity than actually occurred during the Last Glacial Maximum. These studies, however, mostly cover the last glacial–interglacial transition and do not examine periods with intermediate pCO$_2$ such as during the early glacial (MIS 5a–d) or interglacials prior to 430 000 years ago (430 ka). Comparing the vegetation record of subsequent climate cycles showing different CO$_2$ levels might help to better understand the effects of pCO$_2$ on the vegetation.

During the Brunhes Chron (past 780 kyr), the length of the glacial cycles became much longer, lasting roughly 100 kyr due to a strong non-linear response of the ice sheets to solar forcing (Mudelsee and Stattegger, 1997). Model experiments of Ganopolski and Calov (2011) indicate that low atmospheric CO$_2$ concentrations are a prerequisite for the long duration of the glacial cycles of the past 800 kyr. Then, roughly midway through the Brunhes Chron, the amplitude of the climate cycles shifted with a change in the maximum CO$_2$ concentration during interglacials.

This so-called Mid-Brunhes Event (MBE) (Jansen et al., 1986) – also called Mid-Brunhes Transition – occurred about 430 kyr ago and marks the transition between interglacials characterized by rather low atmospheric CO$_2$ around 240 ppm (parts of Marine Isotope Stages (MIS) 19, 17, 15, 13) to interglacials in which CO$_2$ levels reached 270 ppmv or more (parts of MIS 11, 9, 7, 5, 1) (Lüthi et al., 2008; Bereiter et al., 2015). The climate transition of the MBE has been extensively studied using Earth system models of intermediate complexity. Yin and Berger (2010) stress the importance of forcing by austral summer insolation, and Yin and Berger (2012) argue that the model vegetation (tree fraction) was forced by precession through precipitation at low latitudes. Both papers show the necessity to include the change in atmospheric CO$_2$ in the explanation of the MBE (Yin and Berger, 2010, 2012). Yin (2013), however, concludes that it is not necessary to invoke a sudden event around 430 ka to explain the increased interglacial CO$_2$; the differences between interglacials before and after the MBE can be explained by individual responses in Southern Ocean ventilation and deep-sea temperature to various combinations of the astronomical parameters. On the other hand, statistical analysis suggests a dominant role of the carbon cycle, which changed over the MBE (Barth et al., 2018). Paillard (2017) developed a conceptual model of orbital forcing of the carbon cycle in which sea-level fluctuations and the effects on carbon burial are decisive during shifts in the climate system. Further modelling by Bouttes et al. (2018) showed qualitative agreement with the palaeodata of pre- and post-MBE interglacials but largely underestimated the amplitude of the changes. Moreover, the simulated vegetation seems to counteract the effects of the oceanic response (Bouttes et al., 2018). Thus, the vegetation, in particular at low latitudes, may play a crucial but poorly understood role in the climate system.

Comparing records of pre- and post-MBE interglacials could offer insight in the interglacial climate at different levels of CO$_2$ (Foley et al., 1994; Swann et al., 2010). We define interglacials after PAGES (2016) listing MIS 19c, 17c, 15a, 15e and 13a as pre-MBE and MIS 11c, 9e, 7e, 7a–c, 5e and 1 as post-MBE. Currently, only a handful of vegetation records covering the entire Brunhes Chron have sufficient temporal resolution to enable comparisons between interglacials before and after the Mid-Brunhes Transition. These records are from the eastern Mediterranean, the Colombian Andes (PAGES, 2016), west and east Africa (Dupont et al., 1989; Miller and Goslin, 2014; Castañeda et al., 2016a; Johnson et al., 2016; Ivory et al., 2018; Owen et al., 2018). The Andean pollen record is strongly influenced by the immigration of oak from North America during MIS 12 (Torres et al., 2013). For the eastern Mediterranean, a decline in plant diversity is observed at Tenaghi Philippon (Greece) where the modern Mediterranean oak forests gradually emerged in the interglacials after MIS 16 but before the MBE (Tzedakis et al., 2006, 2009). The west African record of Lake Bosumtwi in Ghana allows identification of six forest assemblages since

540 ka related to the interglacials of MIS 13, 11, 9, 7, 5e and 1. The forests' assemblage of MIS 13, however, does not show a strong contrast with those of the interglacials after the MBE (Miller and Goslin, 2014). The marine pollen record of Ocean Drilling Program (ODP) site 658 off Cape Blanc tracks the latitudinal position of the open grass-rich vegetation zones at the boundary between the Sahara and Sahel suggesting shifting vegetation zones between glacials and interglacials (Dupont and Hooghiemstra, 1989; Dupont et al., 1989). The drier interglacials occurred after MIS 9, which indicates a transition after the MBE to more arid conditions. Additionally, stable carbon isotope records from Chinese loess sections indicate interglacial–glacial variability in the C$_3$–C$_4$ proportions of the vegetation (Sun et al., 2010; Lyu et al., 2018). However, the latter records do not show a prominent vegetation shift over the MBE.

For East Africa, two terrestrial records and a marine one are available. From Lake Malawi, Johnson et al. (2016) infer wetter conditions and increased woodland vegetation between 800 and 400 ka based on the stable carbon isotopic composition of plant wax shifting from less to more strongly depleted values. Also from Lake Malawi, Ivory et al. (2018) published a pollen record of the past 600 kyr revealing a number of phases of Miombo woodland and mountain forest alternating with savannah vegetation (dry woodland and wooded grassland). Recently, a new record from Lake Magadi (Kenya) has been published indicating a change from wetter conditions to more aridity after 500 ka, contrasting the Lake Malawi results (Owen et al., 2018). In Lake Magadi, the representation of *Podocarpus* decreased over the MBE, while open grassy vegetation and salinity of the lake increased (Owen et al., 2018). Neither the Lake Malawi nor the Lake Magadi records show dominant interglacial–glacial variability.

The marine record retrieved south of the Limpopo River mouth (core MD96-2048) allows inferences about vegetation and climate in the catchment area of the Limpopo River draining large areas of South Africa, Botswana, Zimbabwe and Mozambique. Based on sediment chemistry, Caley et al. (2018a) reported the effects of increased summer insolation in increased fluvial discharge and variability associated with eccentricity, which modulates precession amplitudes. Superimposed on the orbital-scale precipitation variability, a long-term trend from 1000 to 600 ka towards increased aridity in southeastern Africa was found (Caley et al., 2018a). The plant leaf wax carbon isotopic (hereafter $\delta^{13}C_{wax}$) record of the same core was originally interpreted as reflecting a trend toward increasingly drier glacials and wetter interglacials over the past 800 kyr (Castañeda et al., 2016a). Additionally, the average chain lengths of the plant leaf waxes exhibit a stepwise decrease at 430 ka suggesting a change from more shrub vegetation before the MBE to a larger contribution of trees during the post-MBE interglacials (Castañeda et al., 2016a). Thus, a pollen record of MD96-2048 has the potential to register the changes in

interglacial vegetation cover over the MBE. We might expect a change of Southern Hemisphere vegetation being less ambiguous than the changes found on the Northern Hemisphere (see above), because modelling indicates that the effects of the MBE were more pronounced on the Southern Hemisphere (Yin and Berger, 2010). Until now, the palynology of only the last 350 kyr has been published (Dupont et al., 2011a), and therefore here we extend the pollen record of MD96-2048 to cover the past 800 kyr in sufficient resolution. As described below, our new palynology results have led to the reinterpretation of the MD96-2048 δ^{13}C$_{wax}$ record (Castañeda et al., 2016a).

1.1 Previous work on core MD96-2048

The sediments of MD96-2048 were retrieved in the middle of the Delagoa Bight (Fig. 1) from the southern Limpopo cone forming a depot centre that has been build up at least since the Late Miocene (Martin, 1981). The site collects terrestrial material including pollen and spores mostly from the rivers that discharge into the Delagoa Bight of which the Limpopo River is the biggest draining large areas of northern South Africa and southern Mozambique. Apart from the offshore winds descending from the interior plateau, so-called Berg winds, the predominant wind direction is landward (Tyson and Preston-Whyte, 2000) and aeolian input of terrestrial material is probably minor. Thus, pollen source areas would cover the region north of the Delagoa Bight in southern Mozambique and the region west of the Lebombo hills and the Drakensberg escarpment (Dupont et al., 2011a).

A wide variety of measurements have been performed on MD96-2048 sediments. Caley et al. (2011, 2018a) recorded stable oxygen isotopes of benthic foraminifers (*Planulina wuellerstorfi*) providing a stable oxygen stratigraphy and age model aligned to the global stack LR04 (Lisiecki and Raymo, 2005) for the past 2200 kyr. Trace element (Mg/Ca ratios) of the planktic foraminifer *Globigerinoides ruber sensu stricto* and foraminifer assemblages were combined to produce a robust sea surface temperature (SST) record (Caley et al., 2018a). High-resolution (0.5 cm) X-ray fluorescence (XRF) scanning has been performed over the total core length, of which the iron–calcium ratios, ln(Fe/Ca), were used to estimate fluvial terrestrial input variability (Caley et al., 2018a). At millennial resolution, higher plant leaf wax (*n*-alkane) concentrations and ratios and compound-specific stable carbon isotopes (δ^{13}C$_{wax}$) provided a record of vegetation changes in terms of open versus closed canopy and C$_4$ versus C$_3$ plants of the past 800 kyr (Castañeda et al., 2016a). A very low-resolution leaf wax deuterium isotopic record was generated (Caley et al., 2018a) and, in conjunction with other high-resolution proxies including ln(Fe/Ca), was used to reconstruct rainfall and Limpopo River runoff during the past 2.0 Myr.

1.2 Present-day climate and vegetation

Modern climate is seasonal with the rainy season in summer (November to March). Yearly precipitation ranges from 600 mm in the lowlands to 1400 mm in the mountains, whereby rains are more frequent along the coast under the influence of SSTs (Jury et al., 1993; Reason and Mulenga, 1999). Annual average temperatures range from 24 to 16 °C, but in the highlands clear winter nights may be frosty.

The modern vegetation of this area belongs to the forest, Highveld grassland and savannah biomes and also includes azonal vegetation (Fig. 1) (Dupont et al., 2011a, and references therein). The natural potential vegetation of the coastal belt is forest, although at present it is almost gone; north of the Limpopo River mouth, rain forests belong to the Inhambane phytogeographical mosaic and south of the Limpopo River the forest belongs to the Tongaland–Pondoland regional mosaic (White, 1983). The vegetation of the northern part of the Tongaland–Pondoland region is the Northern Coastal Forest (Mucina and Rutherford, 2006). Semideciduous forest is found in the Lebombo hills (Kersberg, 1996). Afromontane forest and Highveld grasslands grow along the escarpment and on the mountains. The savannahs of the Zambezian phytogeographical region, including, e.g. the Miombo dry forest, occur further inland (White, 1983). Azonal vegetation consists of freshwater swamps, alluvial and seashore vegetation, and mangroves (Mucina and Rutherford, 2006).

2 Material and methods

Pollen analysis of the 37.59 m long core MD96-2048 (26°10′ S, 34°01′ E; 660 m water depth) was extended with 65 samples down core to 12 m (790 ka). Average sampling distance for the Brunhes part was 7 cm reaching an average temporal resolution of 4 kyr according to the age model based on the stable oxygen isotope stratigraphy of benthic foraminifers (Caley et al., 2011, 2018a). Two older windows have been sampled; 20 samples between 15 and 26 m (943–1537 ka) and 19 samples between 30 and 36 m (1785–2143 ka) were taken with an average resolution of 31 and 20 kyr, respectively.

Pollen preparation has been described in Dupont et al. (2011a). In summary, samples were decalcified with hydrochloric acid (HCl) (∼ 10 %), treated with hydrofluoric acid (HF) (∼ 40 %) for 2 d, ultrasonically sieved over an 8 μm screen and, if necessary, decanted. The samples were spiked with two *Lycopodium* spore tablets (either of batch no. 938934 or batch no. 177745). Residues were mounted in glycerol and pollen and spores examined at 400× or 1000× magnification. Percentages are expressed based on the total of pollen and spores ranging from over 400 to 60 – only in six samples this sum amounts to less than 100. Confidence intervals (95 %) were calculated after Maher Jr. (1972, 1981). Pollen has been identified using the reference collec-
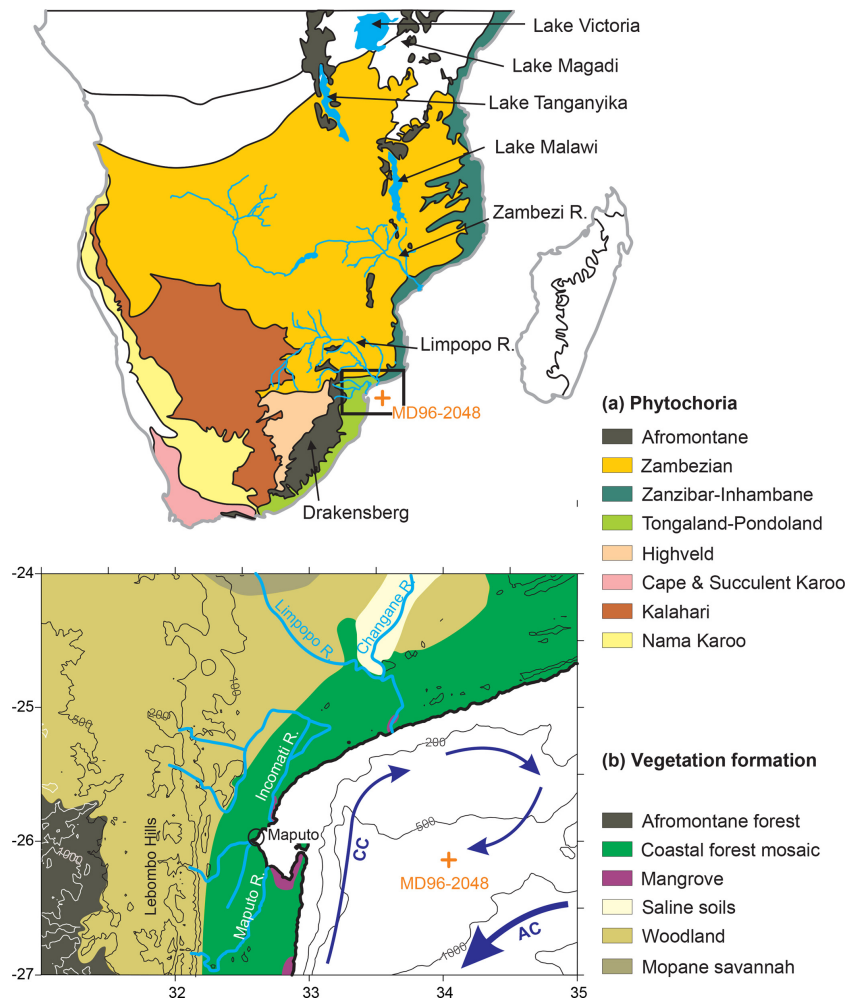
Figure 1. (a) Map of southern Africa with the main phytochoria after White (1983). **(b)** Site location of MD96-2048; main vegetation formations; main rivers; 100, 200, 500 and 1000 m contours; 200, 500 and 1000 m bathymetric contours; Agulhas (AC) and counter current (CC) forming a coastal Delagoa Bight lee eddy. Zambezian vegetation woodland and savannah north of $\sim 25°30'$ S, Tongaland–Pondoland coastal forests south of $\sim 25°30'$ S, Zanzibar–Inhambane coastal forests east of 33–34° E. West of the escarpment with Afromontane forest rises the interior plateau covered with Highveld grasslands.

tion of African pollen grains of the Department of Palynology and Climate Dynamics of the University of Göttingen, the African Pollen Database collection and literature (e.g. Bonnefille and Riollet, 1980; Scott, 1982; Köhler and Brückner, 1982, 1989; Schüler and Hemp, 2016).

We assigned pollen taxa to groups such as riparian, woodland, forest, etc. (Table S1 in the Supplement) using information given by Scott (1982), White (1983), Beentje (1994), Kersberg (1996), Coates Palgrave (2002) and Vincens et al. (2007). Additionally, we carried out a multivariate analysis in the form of an endmember model unmixing procedure (Weltje, 1997), the statistics of which are specifically designed for the treatment of percentage data. We regard the pollen percentages as a series of pollen assemblage mixtures, whereby each modelled endmember may be interpreted as the representation of one or more biomes. This linear mixing model can be compared to a ternary diagram but allowing for more than three axes. We use a version of the unmixing algorithm programmed in MATLAB by David Heslop in 2008. Taxa occurring in six or more samples (listed in Table S2 in the Supplement) were used in the endmember modelling (148 of 231 taxa in 220 samples). We selected a model with four components explaining more than 95 % of the variance ($r^2 = 0.953$). Iteration was stopped at $1000\times$ resulting in a convexity at termination of -1.6881. The significance level at 99 % for taxa to score on the assemblages was 0.018.

To study the correlations between different parameters, we used a linear regression model (least-square regression) on linearly interpolated values (5 kyr steps) from 0 to 790 ka. Correlation coefficients are given in Table 1. For interpolation and testing the correlation, we used the package PAST (Hammer et al., 2001).

Table 1. Correlation coefficients calculated with PAST (Hammer et al., 2001). Significant correlations are underlined (95 %) or bold and underlined (99 %). Average chain length (ACL), ratio of concentrations of $C_{31} / (C_{31} + C_{29})$ and stable carbon isotope composition of the C_{31} n-alkane ($\delta^{13}C_{wax}$) after Castañeda et al. (2016b). Cyperaceae and Poaceae pollen percentages (of total pollen and spores) after Dupont et al. (2011b) and this study. ln(Fe/Ca) data are after Caley et al. (2018c).

r^2	ACL	Ratio $C_{31} / (C_{29} + C_{31})$	$\delta^{13}C_{wax}$ (‰)	Cyperaceae (%)	Poaceae (%)	XRF ln(Fe/Ca)
ACL	1					
Ratio $C_{31} / (C_{31} + C_{29})$	**0.635**	1				
$\delta^{13}C_{wax}$	**0.079**	**0.180**	1			
Cyperaceae (%)	0.027	**0.140**	**0.142**	1		
Poaceae (%)	0.003	0.016	0.003	**0.165**	1	
XRF ln(Fe/Ca)	0.016	0.032	**0.227**	**0.110**	0.011	1

3 Result and discussion

3.1 Terrestrial input and provenance of the C_4 plant wax

Pollen percentages of Cyperaceae (sedges) and Poaceae (grasses) are plotted in Fig. 2 together with the $\delta^{13}C_{wax}$ of the C_{31} n-alkane and XRF-scanning data, ln(Fe/Ca), the natural logarithm of elemental ratios of iron over calcium. Comparing the records of Cyperaceae and $\delta^{13}C_{wax}$ reveals that high relative amounts of C_4 plant material co-varied with increased representation of sedges. They also co-varied with higher terrestrial input indicated by ln(Fe/Ca) and increased precipitation as suggested by deuterium of the C_{31} n-alkane (Caley et al., 2018a). We substantiated the correlations for the Brunhes Chron between pollen percentages, leaf waxes and elemental ratios in Table 1. Leaf wax data are after Castañeda et al. (2016b) including average chain length (ACL) of the C_{27}–C_{33} n-alkanes, the ratio of $C_{31} / (C_{31} + C_{29})$ and $\delta^{13}C_{wax}$. XRF ln(Fe/Ca) ratios are from Caley et al. (2018c). Significant correlation is found between the leaf wax parameters and Cyperaceae data but not between $\delta^{13}C_{wax}$ (indicative of C_4 inputs) and Poaceae pollen percentages – although a correlation exists between Cyperaceae and Poaceae percentages. While the sedge pollen percentages fluctuate between 10 % and 50 % (mostly > 20 %), the percentages of grass pollen are always lower than 20 %. Such low grass pollen values have not been found adjacent C_4 grass dominated biomes (mainly savannahs) on the western side of the continent (Dupont, 2011). It is, therefore, likely that in sediments of MD96-2048 the C_4 component of the plant wax originated from C_4 sedges rather than from C_4 grasses.

South Africa has 68 species of Cyperaceae (sedges) of which 28 use the C_4 pathway (among the 10 *Cyperus* species, 8 are C_4) predominantly growing in the northern part of the country (Stock et al., 2004). They are an important constituent of tropical swamps and riversides (Chapman et al., 2001). An inventory of six modern wetlands between 500 and 1900 m in KwaZulu-Natal shows that C_4 grasses dominate the dry surroundings of the wetlands at all altitudes (Kotze and O'Connor, 2000). In the wet parts of the wetlands, how-

ever, C_4 sedges may make up to 60 % of the vegetation cover at 550 m. At higher altitudes the coverage of C_4 sedges declines (Kotze and O'Connor, 2000).

Cyperaceae pollen concentration (Fig. 3) and percentages correlate with ln(Fe/Ca) and with $\delta^{13}C_{wax}$ (Table 1, Fig. 2). The ratios of terrestrial iron over marine calcium can be interpreted as a measure for terrestrial input, which in this part of the ocean is mainly fluvial. Correlation between increased fluvial discharge and increased C_4 vegetation as well as increased Cyperaceae pollen has been reported from sediments off the Zambezi (Schefuß et al., 2011; Dupont and Kuhlmann, 2017). Moreover, a fingerprint of C_4 sedges was found in Lake Tanganyika (Ivory and Russel, 2016). As a consequence, material (leaf waxes and pollen) from the riverine vegetation is probably better represented than that from dry and upland vegetation. These results corroborate the reinterpretation of the $\delta^{13}C_{wax}$ record, in which the increased representation of C_4 plants (n-alkanes enriched in ^{13}C) is instead attributed to stronger transport of material from the upper Limpopo catchment and the extension of swamps containing C_4 sedges under more humid conditions (Caley et al., 2018a). Previously, Castañeda et al. (2016a) had interpreted increased C_4 inputs as reflecting increased aridity.

Relatively low values of Cyperaceae pollen and Fe/Ca ratios are found for most interglacials of the Brunhes Chron (Figs. 2 and 3), which could be interpreted as an effect of sea-level highstands. However, Caley et al. (2018a) demonstrated that the fluvial discharge is not related to sea-level changes. From the bathymetry of Delagoa Bight, a strong influence of sea level is also not expected because the shelf is not broad and the locality of core MD96-2048 is relatively remote on the Limpopo cone in the centre of the clockwise flowing Delagoa Bight lee eddy. The eddy transports terrestrial material northeastwards before it is taken southwards (Fig. 1) (Martin, 1981) and likely has not changed direction during glacial times. Thus, fluvial discharge was probably low during interglacials (among other periods), which might be the combined result of more evapotranspiration and less precipitation. Despite drier conditions, the representation of woodland and dry
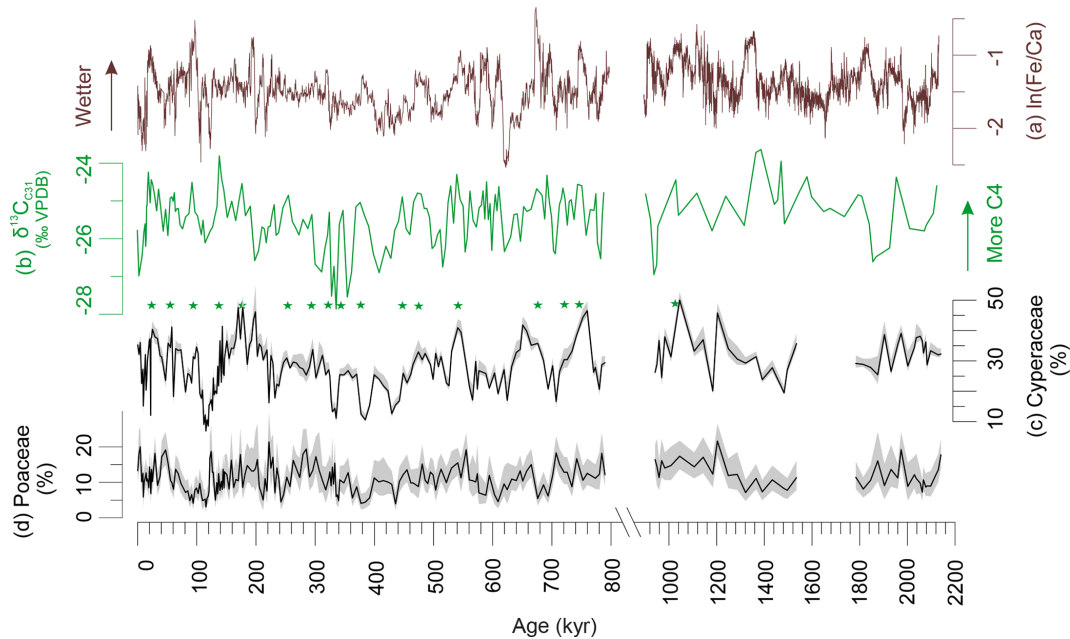
Figure 2. Indicators of C$_4$ vegetation and terrestrial input. **(a)** Elemental Fe/Ca ratios (Caley et al., 2018c); less negative values indicate relatively wetter conditions. **(b)** δ^{13}C$_{wax}$ of the *n*-alkane C$_{31}$ (Castañeda et al., 2016b; Caley et al., 2018e); less negative values of around -24‰ indicate more C$_4$ inputs while more negative values of around -28‰ indicate more C$_3$ inputs. **(c)** Cyperaceae (sedges) pollen percentages (Dupont et al., 2011b, this study). **(d)** Poaceae (grass) pollen percentages (Dupont et al., 2011b, this study). Shaded areas denote 95 % confidence intervals after Maher Jr. (1972). Stars denote corresponding maxima in Cyperaceae pollen percentages and the stable carbon isotopes indicating C$_4$ vegetation. VPDB: Vienna Pee Dee Belemnite. Note the scale break.

forest is relatively high during the interglacial periods (Fig. 3; see also next section).

3.2 Endmembers representing vegetation on land

Palynological results have been published for the past 350 kyr (Dupont et al., 2011a) providing a detailed vegetation record for the past three climate cycles. Pollen and spore assemblages could be characterized initially by three endmembers via endmember modelling (EM1, EM2, EM3). The assemblage of EM1 was dominated by *Podocarpus* (yellow wood) pollen percentages being more abundant during the non-interglacial parts of MIS 5, 7 and 9. EM2 was characterized by pollen percentages of Cyperaceae (sedges), Ericaceae (heather) and other plants of open vegetation and abundant during full glacial stages. EM3 constituted of pollen from woodland, forest and coastal vegetation and was interpreted to represent a mix of several vegetation complexes.

We repeated the endmember modelling for the extended record covering the entire Brunhes Chron and the two early Pleistocene windows. The analysis of the extended dataset gave compatible results with the previous analysis (Dupont et al., 2011a). The main difference is that the longer sequence allowed to distinguish two assemblages of interglacial vegetation. In terms of analysis, the cumulative increase of explanatory power lessened after four (instead of three) endmembers, and a model with four endmembers was cho-

sen. We used the scores of the different pollen taxa on the endmember assemblages for our interpretation of the endmembers (list of taxa and scores in Tables S1 and S2 in the Supplement). This interpretation is summarized in Table 2. To distinguish between the previous and current analyses (which show strong similarities), we have given new names to the endmember assemblages reflecting our interpretation: E-heathland, E-Mountain-Forest, E-Shrubland and E-Woodland. A selection of pollen percentage curves are plotted together with each endmember's fractional abundance in Figs. S2–S5 in the Supplement.

E-Heathland. Of the four endmember assemblages (Fig. 3), one endmember had a counterpart in EM2 (Dupont et al., 2011a) of the previous analysis. Not only composition but also the fractional abundances, which were high during glacial stages, are very much alike. We name this endmember "E-Heathland", which is dominated by Cyperaceae (sedges) pollen percentages, followed by Ericaceae (heather) pollen and hornwort (Anthocerotaceae) spores (Table 2). Also *Lycopodium* (clubmoss) spore, Restionaceae and *Stoebe*-type pollen percentages score highest on this endmember. The E-Heathland assemblage represents a fynbos-like open vegetation growing during full glacials. Other pollen records from SE Africa also indicate an open ericaceous vegetation with sedges and Restionaceae during glacial
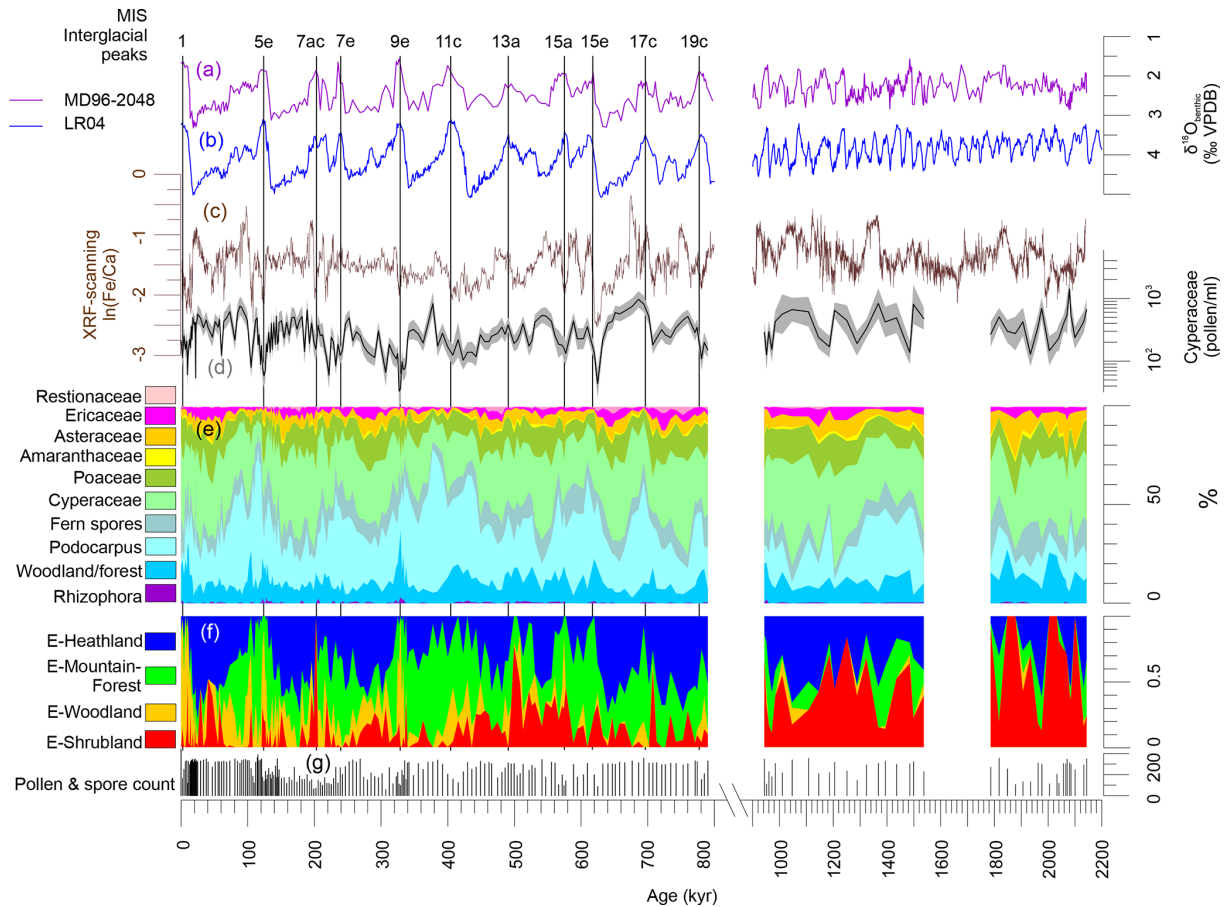
Figure 3. Summary of results of MD96-2048. **(a)** Stable oxygen isotopes of benthic foraminifers of core MD96-2048 (Caley et al., 2018b). **(b)** Global stack of stable oxygen isotopes of benthic foraminifers, LR04 (Liesiecki and Raymo, 2005). **(c)** Elemental ratios ln(Fe/Ca). **(d)** Cyperaceae pollen concentration per mililitre (shading denote 95 % confidence intervals after Maher Jr., 1981). **(e)** Pollen summary diagram (woodland and forest taxa are listed in Table S1 in the Supplement). **(f)** Fractional abundance of endmembers E-Heathland, E-Mountain-Forest, E-Woodland and E-Shrubland. **(g)** Pollen and spore count used to calculate percentages. On top interglacial peaks after PAGES (2016) are indicated. VPDB: Vienna Pee Dee Belemnite.

times (Scott, 1999; Dupont and Kuhlmann, 2017). The record of MD96-2048 testifies that this type of open glacial vegetation has regularly occurred for at least 2 million years.

E-Mountain-Forest. Like the endmember EM1 (Dupont et al., 2011a) of the previous analysis, one endmember is dominated by *Podocarpus* (yellow wood) pollen percentages (Table 2). The assemblage is enriched by pollen of *Celtis* (hackberries) and *Olea* (olive trees) accompanied by undifferentiated fern spores. The interpretation as an assemblage representing mountain forest is rather straightforward, and we name the assemblage "E-Mountain-Forest". The fractional abundance of the E-Mountain-Forest is also high in glacials of the Brunhes Chron but not during the extreme glacial stages, when temperatures and *p*CO$_2$ are particularly low (Fig. 3). It is low in the early Pleistocene parts of the record.

E-Shrubland. The remaining endmember assemblages have no direct counterpart in the previous analysis, although summed together the pattern of fractional abundance is similar to that of EM3 (Dupont et al., 2011a). One endmember groups together 44 pollen taxa, mostly from coastal and dune vegetation, which we name "E-Shrubland". It includes pollen of Asteraceae and Poaceae (grasses). The latter are not very specific as grass pollen values score almost as high on other endmember assemblages (E-Heathland and E-Woodland). Several taxa scoring on this endmember are known from coastal or halophytic settings such as *Gazania* type, Amaranthaceae, *Tribulus*, Acanthaceae and *Euphorbia* type. Arboreal taxa in this assemblage are *Dombeya*, *Acacia* and Meliaceae/Sapotaceae (Table 2). The most typical taxa are the *Buxus* species. We distinguished three types of *Buxus* pollen: *B. macowanii* type, *B. hildebrandtii* type and *B.* cf. *madagascarica* (Köhler

and Brückner, 1982, 1989). *B. madagascarica* grows on Madagascar and its pollen is only found sporadically, while the other two species inhabit bushland and forest on coastal dunes of the east African mainland. *B. hilde-brandtii* nowadays is found in Somalia and Ethiopia, and *B. macowanii* is native in South Africa. The record of M96-2048 indicates that these *Buxus* species were more common in the early Pleistocene than during the Brunhes Chron (Fig. 3).

E-Woodland. The last endmember, which we name "E-Woodland", groups together 39 pollen taxa from forest and woodland species with maximum values of less than 5 % or 2 % of the total of pollen and spores. To this assemblage belong *Pseudolachnostylis*, *Dodonaea viscosa* and *Manilkara*, which are woodland trees. *Protea* (sugarbush) and *Myrsine africana* (Cape myrtle) grow more upland, and *Alchornea* is a pioneer forest tree often growing along rivers. Others include wide-range woodland taxa such as Combretaceae species. The occurrence of pollen of *Brachystegia* (Miombo tree), *Burkea africana*, *Spirostachys africana* and *Hymenocardia* in this assemblage is indicative of Miombo dry forest and woodland. The assemblage additionally includes Rhizophoraceae pollen from the coastal mangrove forest (Table 2). The fractional abundance of the E-Woodland assemblage is low during the early Pleistocene, increased during the interglacials prior to the MBE and had maximum values during Interglacials 9e, 5e and 1 (Figs. 3, 4). These interglacials also exhibited maximum percentages of arboreal pollen excluding *Podocarpus*.

In summary, the endmember analysis indicates a very stable open ericaceous vegetation with partially wet elements such as sedges and Restionaceae characterizing the landscape of full glacials (when global temperatures and pCO_2 were lowest). During the less extreme parts of the glacials, mountain *Podocarpus* forest was extensive as in most mountains of Africa (Dupont, 2011; Ivory et al., 2018). On the other hand, interglacials were characterized by coastal shrubs. In the course of the Brunhes, the woody component, which was relatively weak before the MBE, became more and more important, reflecting the same long-term trend found in the leaf wax records (Castañeda et al., 2016a). It is likely that the Miombo dry forest and woodland migrated into the region in the successive interglacials of the Brunhes Chron. Particularly during Interglacials 9e and 1, the area might have been more forested than during the older interglacials of the Brunhes Chron.

3.3 Long-term trends in vegetation and climate of east Africa

The region of the Limpopo River becoming more and more wooded in the course of successive interglacials (Castañeda

Table 2. Interpretation of the endmembers.

Endmember	Main pollen taxa
E-Heathland	Cyperaceae, Ericaceae, *Phaeoceros*, Restionaceae, *Stoebe* type, *Anthoceros*, *Typha*, *Lycopodium*, Restionaceae
E-Mountain-Forest	*Podocarpus*, *Celtis*, *Olea*
E-Shrubland	Poaceae, Asteroideae, *Buxus*, Amaranthaceae, *Euphorbia*, Meliaceae–Sapotaceae, *Acacia*, *Riccia* type, *Tribulus*, Acanthaceae pp., Asteraceae Vernoniae, *Hypoestes–Dicliptera* type, *Gazania* type, *Dombeya*
E-Woodland	*Alchornea*, *Spirostachys africana*, *Pteridium* type, Polypodiaceae, *Myrsine africana*, *Cassia* type, Rhizophoraceae, Aizoaceae, Combretaceae pp., *Manilkara*, *Burkea africana*, *Brachystegia*, *Dodonaea viscosa*, *Pseudolachnostylis*, *Hymenocardia*, *Aloe*, Rhamnaceae pp., *Protea*, *Parinari*

et al., 2016a) somewhat paralleled the conditions around Lake Malawi (Johnson et al., 2016). However, around Lake Malawi, forested phases of either mountain forest, seasonal forest or Miombo woodland alternating with savannahs occurred during both glacial and interglacial stages (Ivory et al., 2018). Also in contrast to the Lake Malawi record, the MD96-2048 Poaceae pollen percentages fluctuated little and remained relatively low (less than 20 %), indicating that savannahs were of less importance in the Limpopo catchment area and the coastal region of southern Mozambique.

The trend to increased woodland in SE Africa after the MBE, noted at both Lake Malawi and in the Limpopo River catchment (Johnson et al., 2016; Caley et al., 2018a, this study), contrasts with the trend around Lake Magadi at the Equator. At Lake Magadi, a trend to less forest marks the Mid-Brunhes Transition (Owen et al., 2018). Antiphase behaviour of SE African climate with that of west and east Africa emphasizes the importance of the average position of the tropical rain belt shifting southwards during globally cold periods as has been inferred from Holocene to last glacial records of Lake Malawi (Johnson et al., 2002; Scholz et al., 2011). Our results confirm this relationship existed over the entire Brunhes Chron.

The Lake Malawi pollen records and Lake Magadi pollen records in Kenya (Johnson et al., 2016; Owen et al., 2018) do not show much of a glacial–interglacial rhythm and are dominated by the precession variability in tropical rainfall (e.g. Clement et al., 2004). Obviously, in the tropical climate of the Southern Hemisphere north of $\sim 15°$ S, the hydrological regime had more effect on the vegetation than changes
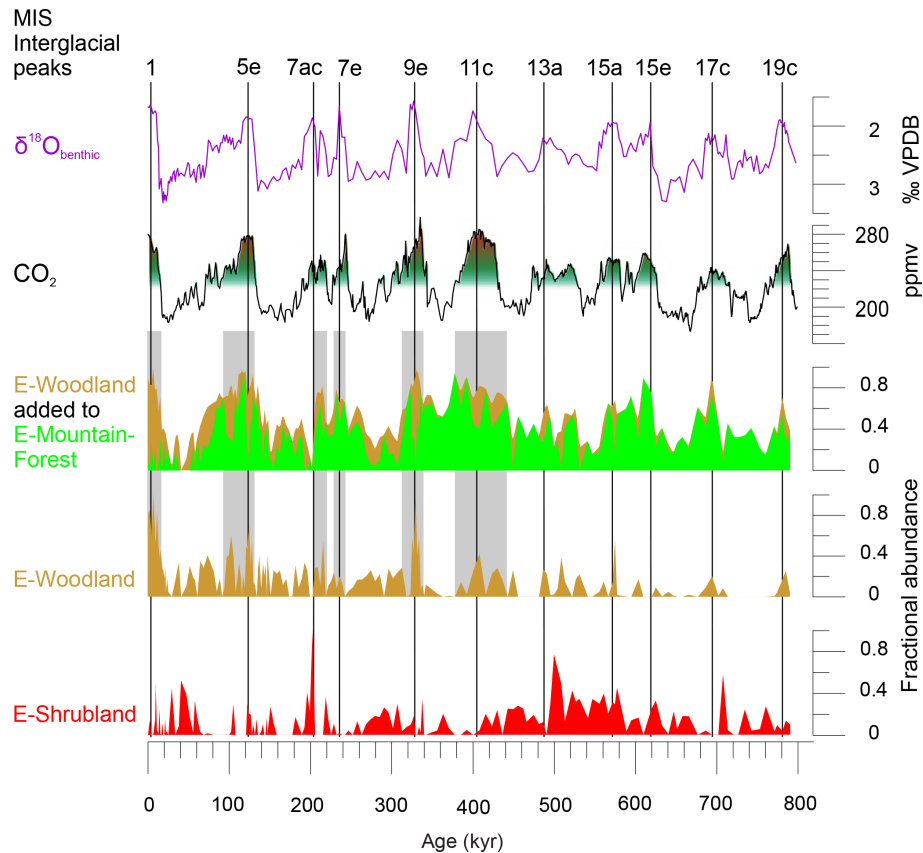
Figure 4. Comparing pollen assemblages E-Mountain-Forest, E-Woodland and E-Shrubland with atmospheric CO$_2$ (Bereiter et al., 2015; PAGES, 2016). On top are denoted interglacial peaks of the past 800 kyr (PAGES, 2016) and stable oxygen isotopes of benthic foraminifera (δ^{18}O$_{benthic}$) of MD96-2048 (Caley et al., 2018b). CO$_2$ levels of 220 and 270 ppmv are indicated with green–red shading. Grey shading highlights periods with maximum atmospheric CO$_2$ and maximum values of the sum of E-Woodland and E-Mountain-Forest. VPDB: Vienna Pee Dee Belemnite.

in temperature, while further south the impact of glacial–interglacial variability on the vegetation increased.

3.4 Effects of atmospheric pCO$_2$

While the hydroclimate of the region shows precession variability (Caley et al., 2018a), the vegetation shows a glacial–interglacial rhythm (Fig. S1 in the Supplement), indicating that besides hydrology, temperature and/or atmospheric CO$_2$ levels were important drivers of the vegetation development. Combining the results of the pollen assemblages with stable carbon isotopes and elemental information indicates that during interglacials the region of SE Africa (northern South Africa, Zimbabwe and southern Mozambique) was less humid. This is in accordance with other palaeoclimate estimates for the region (see reviews by Simon et al., 2015; Singarayer and Burrough, 2015).

The interglacial woodlands (represented by E-Woodland, Fig. 4) would probably have grown under warmer and drier conditions than the glacial mountain forest (represented by E-Mountain-Forest). The increase in maximum pCO$_2$ levels

during the post-MBE interglacials might have favoured tree growth, as higher pCO$_2$ levels would have allowed decreased stomatal conductivity and thus relieved drought stress (Jolly and Haxeltine, 1997). Woodlands would have expanded at the cost of mountain forest during MIS 11c, 9e, 5e and 1, and to a lesser extent during 7e and 7c, when temperatures and pCO$_2$ were high (Fig. 4). It might be only after interglacial pCO$_2$ levels rose over $\sim$ 270 ppmv that Miombo woodland could fully establish in the area during the warm and relatively dry post-MBE interglacials.

The glacial stages showed the expansion of either mountain forest or heathland. The record indicates extension of mountain forests in SE Africa during those parts of the glacial stages with low temperatures and atmospheric pCO$_2$ exceeding $\sim$ 220 ppmv (Fig. 5). If low temperatures were the only driver of the extension of mountain forests, further spread into the lowlands during the coldest glacial phases should be expected. Instead, when pCO$_2$ dropped below $\sim$ 220 ppmv during those colder glacial periods, mountain forest declined, in particular during MIS 18, 16, 14, 8, 6 and 2. A picture emerges of cool glacial stages in SE Africa in
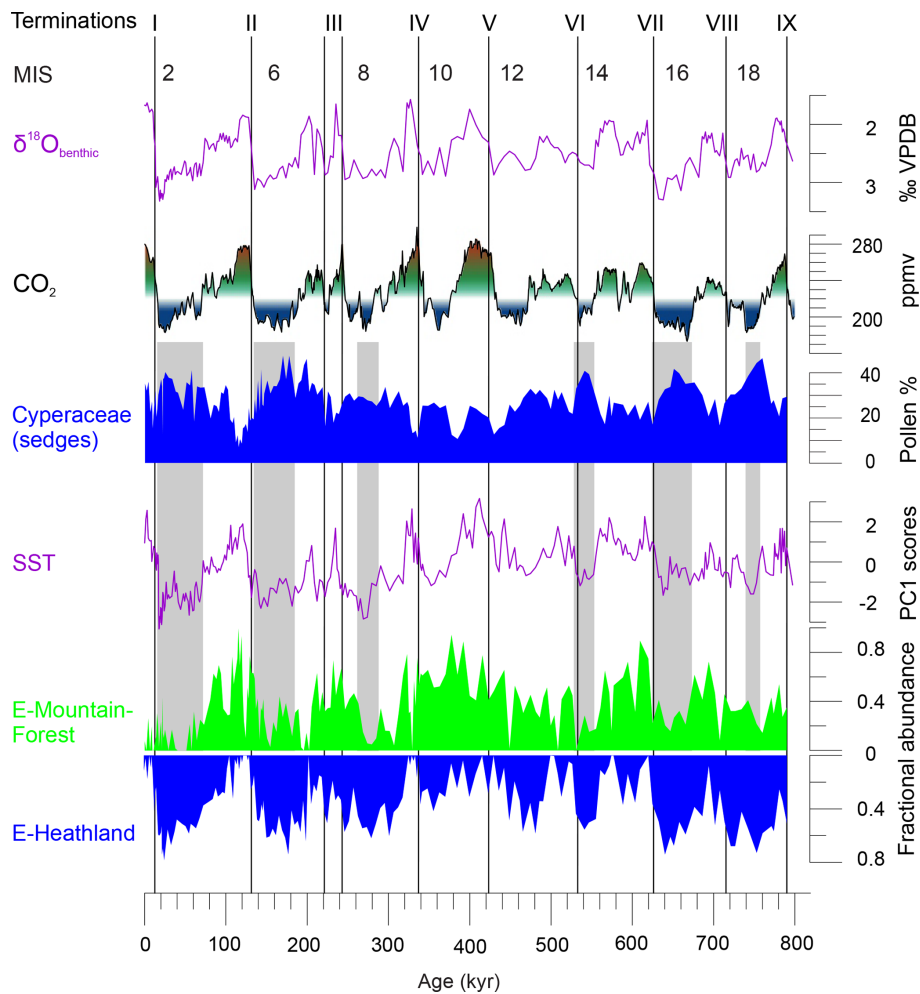
Figure 5. Comparing Cyperaceae pollen percentages and fractional abundances of the glacial pollen assemblages E-Mountain-Forest and E-Heathland with atmospheric CO$_2$ (Bereiter et al., 2015; PAGES, 2016) and sea surface temperatures of the southeastern Indian Ocean (SST PC1 scores of MD96-2048) (Caley et al., 2018d). On top are denoted terminations I through to IX of the past nine glaciations, even-numbered marine isotope stages (MISs), and stable oxygen isotopes of benthic foraminifera (δ^{18}O$_{benthic}$) of MD96-2048 (Caley et al., 2018b). CO$_2$ levels of 220 and 270 ppmv are indicated with blue–green–red shading. Grey shading highlights periods with minimum atmospheric CO$_2$, minimum values of E-Mountain-Forest and maximum values of E-Heathland and Cyperaceae pollen. VPDB: Vienna Pee Dee Belemnite.

which tree cover broke down when atmospheric pCO$_2$ became too low. Additionally, mountain forests were important during Interglacials 19c, 17c, 15e, 15a, 13a and 7e, in which pCO$_2$ and Antarctic temperatures were subdued.

With an inverse modelling technique, Wu et al. (2007) estimated the climate inputs for the vegetation model BIOME4 using as information the biome scores of pollen records from equatorial east African mountains. Wu et al. (2007) found that lowering of the tree line under glacial conditions (1–3 °C lower temperatures, less precipitation, 200 ppmv pCO$_2$) depended hardly on temperature but primarily on increased aridity and somewhat on lower pCO$_2$, whereby lower pCO$_2$ amplified the effects of water limitation. However, Izumi and Lézine (2016) found contrasting results using pollen records of mountain sites on both sides of the Congo basin. At any

rate, the lack of trees in the southeast African mountains during glacial extremes is unlikely the result of drought, because our record indicates that climate conditions in SE Africa were less dry during glacials than during interglacials (the post-MBE interglacials in particular). Instead, C$_4$ sedges being an important constituent of the ericaceous fynbos-like vegetation increased during glacials when atmospheric pCO$_2$ and temperatures were low (Fig. 5). However, low temperatures are not particularly favourable for C$_4$ sedges as indicated by the altitudinal distribution of C$_4$ sedges in modern wetlands of KwaZulu-Natal (Kotze and O'Connor, 2000). We presume, therefore, that the extension of C$_4$ sedges during the colder phases of the glacials is the result of low atmospheric CO$_2$ concentrations rather than of low temperatures.

Pollen records of ericaceous vegetation suggest an extensive open vegetation existing in the east African mountains (e.g. Coetzee, 1967; Bonnefille and Riollet, 1988; Marchant et al., 1997; Debusk, 1998; Bonnefille and Chalié, 2000) and in SE Africa and Madagascar (e.g. Botha et al., 1992; Scott, 1999; Gasse and Van Campo, 2001; Scott and Tackeray, 1987) during the last glacial. In our study, ericaceous fynbos-like vegetation (E-Heathland) was found for those parts of the glacials having lower (less than ∼ 220 ppmv) atmospheric pCO$_2$ (Fig. 5). Exceptions were found for MIS 12 and 14 when the difference of pCO$_2$ with that of the preceding stage was small (Bereiter et al., 2015). Dupont et al. (2011a) argued that increase of C$_4$ vegetation as the result of low pCO$_2$ was unlikely because no extension of grasses was recorded. However, this argument is flawed if sedges dominantly constituted the C$_4$ vegetation in the area. We also note that in many parts of South Africa, no substantial increase of C$_4$ grasses occurred but that many sites suggest an expansion of C$_3$ grasses during the Last Glacial Maximum (Scott, 2002).

As climate was wetter during most of the glacials in this part of the world, the question arises about the climatic implication of the ericaceous fynbos-like vegetation (represented by E-Heathland, Fig. 5) extending during full glacials over the mountains of South Africa – and correlating with the SST record (see also the correlation between SST and EM2 in Dupont et al., 2011a). The correlation with SST, however, is problematic. Singarayer and Burrough (2015) argued that the control of the Indian Ocean SSTs on the precipitation of South Africa shifted from a positive correlation during the interglacial to a negative correlation during the Last Glacial Maximum. They invoked the effects of the exposure of the Sunda Shelf (Indonesia) and Sahul Shelf (Australia) on the Walker circulation causing a wetter region over the western Indian Ocean but also weaker easterly winds to transport moisture inland. To question the link between SST and precipitation in SE Africa even further, Caley et al. (2018a) found that the precession signature in the river discharge proxy (ln(Fe/Ca); see also Fig. S1 in the Supplement) was absent in the SST record from the same core. SE Africa would have been more humid during glacials when the temperature difference between land and sea increased.

The increase in C$_4$ vegetation during relative cool and humid climate would be in conflict with the idea that C$_4$ plants are more competitive in hot and dry climates (Ehleringer et al., 1997; Sage, 2004). However, this idea is mainly based on the ecology of grasses and the development of savannahs, while the C$_4$ vegetation expansion in SE Africa during cool and humid phases seems to be driven by sedges. A survey of the distribution of C$_4$ sedges in South Africa revealed that those Cyperaceae do not have the same temperature constraints as C$_4$ grass species (Stock et al., 2004). More important, South African C$_4$ sedges appear to have evolved under wetland conditions rather than under aridity. C$_4$ *Cyperus* species even occur in the wettest parts of lower-altitude wetlands in KwaZulu-Natal (Kotze and O'Conner, 2000).

4 Conclusions

Palynology in combination with sediment chemistry and carbon isotope analysis of leaf waxes carried out on the marine sediments of MD96-2048 retrieved from the Limpopo River cone in the Delagoa Bight (SE Africa) allowed a detailed reconstruction of the biome developments over the Brunhes Chron and comparison with earlier Pleistocene vegetation of SE Africa.

Using endmember modelling, we could distinguish four pollen assemblages: E-Heathland, E-Mountain-Forest, E-Shrubland and E-Woodland. The open sedge-rich and ericaceous vegetation represented by E-Heathland occurred during those parts of the glacials with lower temperatures and atmospheric pCO$_2$. *Podocarpus*-rich mountain forest represented by E-Mountain-Forest extended during the less extreme parts of the glacials. E-Shrubland represents a shrub-like vegetation with coastal elements and *Buxus* species and mainly occurred during the earlier Pleistocene (before 1 Ma). E-Woodland represents interglacial woodlands, Miombo woodland in particular, becoming more and more important in the successive interglacial stages of the Brunhes Chron and dominated the post-MBE interglacials.

Our results indicate the influence of atmospheric pCO$_2$ fluctuations on the shaping of the biomes in SE Africa during the Brunhes Chron. We argue that (1) the precessional rhythms of river discharge compared to the interglacial–glacial biome variability indicate that hydroclimate cannot be the only driver of vegetation change. The other options of forcing mechanisms on interglacial–glacial timescales are temperature and pCO$_2$. (2) Because of the correlation between Cyperaceae pollen percentages and δ^{13}C$_{wax}$ and the lack of correlation between Poaceae percentages and δ^{13}C$_{wax}$ in combination with the relatively low grass pollen percentages, we deduce that the C$_4$ plant imprint mainly derives from the sedges. (3) The expansion of C$_4$ sedges during the colder periods of the glacials is unlikely to result from lower temperatures. Thus, during the colder phases of the glacials, low atmospheric pCO$_2$ might have favoured the expansion of C$_4$ sedges. (4) The expansion of mountain forest during the glacial periods with moderate temperatures and moderate pCO$_2$, and the lack of extension into the lowlands of mountain forest during the colder periods, suggests that low pCO$_2$ became restrictive to the forest. Mountain forests could thrive during glacials as long as pCO$_2$ levels exceeded ∼ 220 ppmv. (5) Based on the elemental composition as a proxy for river discharge [ln(Fe/Ca)], we recognize the post-MBE interglacials as the drier intervals of the sequence. Nevertheless, woodland extended during those periods, which we attribute to increased temperatures and pCO$_2$. Atmospheric pCO$_2$ levels over 250 ppmv might have been a prerequisite

for the expansion of the Miombo woodlands into SE Africa during the post-MBE interglacials.

The vegetation record of the Limpopo catchment area shows a greater impact of glacial–interglacial variability, mainly driven by CO_2 fluctuations, and less influence of hydroclimate compared to the more equatorial records of Lake Malawi and Lake Magadi. The long-term trend of increased woodiness in the course of the Brunhes Chron paralleled that of Lake Malawi but contrasted Lake Magadi, suggesting a long-term southward shift in the average position of the tropical rain belt.

References

Barth, A. M., Clark, P. U., Bill, N. S., He, F., and Pisias, N. G.: Climate evolution across the Mid-Brunhes Transition, Clim. Past, 14, 2071–2087, https://doi.org/10.5194/cp-14-2071-2018, 2018.

Beentje, H.: Kenya trees, shrubs and lianas, National Museum of Kenya, Nairobi, Kenya, 722 pp., 1994.

Bereiter, B., Eggleston, S., Schmitt, J., Nehrbass-Ahles, C., Stocker, T. F., Fischer, H., Kipfstuhl, S., and Chappelaz, J.: Revision of the EPICA Dome C CO_2 record from 800 to 600 kyr before present, Geophys. Res. Lett., 42, 542–549, https://doi.org/10.1002/2014GL061957, 2015.

Bonnefille, R. and Chalié, F.: Pollen-inferred precipitation time-series from equatorial mountains, Africa, the last 40 kyr BP, Global Planet. Change, 26, 25–50, https://doi.org/10.1016/S0921-8181(00)00032-1, 2000.

Bonnefille, R. and Riollet, G.: Pollens des savanes d'Afrique orientale, Éditions du Centre National de la Recherche Scientifique, Paris, France, 140 pp., 1980.

Bonnefille, R. and Riollet, G.: The Kashiru pollen sequence (Burundi). Palaeoclimatic implications for the last 40 000 yr BP in tropical Africa, Quaternary Res., 30, 19–35, https://doi.org/10.1016/0033-5894(88)90085-3, 1988.

Botha, G. A., Scott, L., Vogel, J. C., and Von Brunn, V.: Palaeosols and palaeoenvironments during the Late Pleistocene Hypothermal in northern Natal, S. Afr. J. Sci., 88, 508–512, 1992.

Bouttes, N., Swingedouw, D., Roche, D. M., Sanchez-Goni, M. F., and Crosta, X.: Response of the carbon cycle in an intermediate complexity model to the different climate configurations of the last nine interglacials, Clim. Past, 14, 239–253, https://doi.org/10.5194/cp-14-239-2018, 2018.

Caley, T., Kim, J.-H., Malaizé, B., Giraudeau, J., Laepple, T., Caillon, N., Charlier, K., Rebaubier, H., Rossignol, L., Castañeda, I. S., Schouten, S., and Sinninghe Damsté, J. S.: High-latitude obliquity as a dominant forcing in the Agulhas current system, Clim. Past, 7, 1285–1296, https://doi.org/10.5194/cp-7-1285-2011, 2011.

Caley, T., Extier, T., Collins, J. A., Schefuß, E., Dupont, L., Malaizé, B., Rossignol, L., Souron, A., Mcclymont, E. L., Jiminez-Espejo, F. J., García-Comas, C., Eynaud, F., Martinez, P., Roche, D. M., Jorry, S. J., Charlier, K., Wary, M., Gouvers, P.-Y., Billy, I., and Giraudeau, J.: A two-million-year-long hydroclimatic context for hominin evolution in southeastern Africa, Nature, 560, 76–79, https://doi.org/10.1038/s41586-018-0309-6, 2018a.

Caley, T., Extier, T., Collins, J. A., Schefuß, E., Dupont, L. M., Malaizé, B., Rossignol, L., Souron, A., McClymont, E. L., Jiménez-Espejo, F. J., García-Comas, C., Eynaud, F., Martinez, P., Roche, D. M., Jorry, S., Charlier, K., Wary, M., Gourves, P.-I., Billy, I., and Giraudeau, J.: Planulina wuellerstorfi δ^{18}O analyses of sediment core MD96-2048, https://doi.org/10.1594/PANGAEA.895364, PANGAEA, 2018b.

Caley, T., Extier, T., Collins, J. A., Schefuß, E., Dupont, L. M., Malaizé, B., Rossignol, L., Souron, A., McClymont, E. L., Jiménez-Espejo, F. J., García-Comas, C., Eynaud, F., Martinez, P., Roche, D. M., Jorry, S., Charlier, K., Wary, M., Gourves, P.-I., Billy, I., and Giraudeau, J.: XRF ln(Fe/Ca) record of sediment core MD96-2048, https://doi.org/10.1594/PANGAEA.895361, PANGAEA, 2018c.

Caley, T., Extier, T., Collins, J. A., Schefuß, E., Dupont, L. M., Malaizé, B., Rossignol, L., Souron, A., McClymont, E. L., Jiménez-Espejo, F. J., García-Comas, C., Eynaud, F., Martinez, P., Roche, D. M., Jorry, S., Charlier, K., Wary, M., Gourves, P.-I., Billy, I., and Giraudeau, J.: SST first principal component of sediment core MD96-2048, https://doi.org/10.1594/PANGAEA.895362, PANGAEA, 2018d.

Caley, T., Extier, T., Collins, J. A., Schefuß, E., Dupont, L. M., Malaizé, B., Rossignol, L., Souron, A., McClymont, E. L., Jiménez-Espejo, F. J., García-Comas, C., Eynaud, F., Martinez, P., Roche, D. M., Jorry, S., Charlier, K., Wary, M., Gourves, P.-I., Billy, I., and Giraudeau, J.: Stable carbon isotopes of sediment core MD96-2048, https://doi.org/10.1594/PANGAEA.895357, PANGAEA, 2018e.

Castañeda, I. S., Caley, T., Dupont, L., Kim, J.-H., Malaizé, B., and Sschouten, S: Middle to Late Pleistocene vegetation and climate change insubtropical southern East Africa, Earth Planet. Sc. Lett., 450, 306–316, https://doi.org/10.1016/j.epsl.2016.06.049, 2016a.

Castañeda, I. S., Caley, T., Dupont, L. M., Kim, J.-H., Malaizé, B., and Schouten, S.: Plant leaf wax (n-alkane) data from sediment core MD96-2048, https://doi.org/10.1594/PANGAEA.863919, PANGAEA, 2016b.

Chapman, L. J., Balirwa, J., Bugenyi, F. W. B., Chapman, C., and Crisman, T. L.: Wetlands of East Africa: biodiversity, exploitation, and policy perspectives, edited by: Gopal, B., Junk, W. J., and Davis, J. A., Biodiversity in Wetlands: Assessment, Funktion and Conservation, Backhuys Publishers, Leiden, the Netherlands, 2, 101–131, 2001.

Clement, A. C., Hall, A., and Brocoli, A. J.: The importance of precessional signals in the tropical climate, Clim. Dynam., 22, 327–341, https://doi.org/10.1007/s00382-003-0375-8, 2004.

Coates Palgrave, K.: Trees of Southern Africa, 3rd edition, revised and updated, Struik, Cape Town, South Africa, 1212 pp., 2002.

Coetzee, J. A.: Pollen analytical studies in east and southern Africa, Palaeoecol. Afr., 3, 146 pp., 1967.

Cowling, S. A. and Sykes, M.: Physiological significance of low atmospheric CO$_2$ for plant-climate interactions, Quaternary Res., 52, 237–242, https://doi.org/10.1006/qres.1999.2065, 1999.

Debusk, G. H.: A 37 500-year pollen record from Lake Malawi and implications for the biogeography of afromontane forests, J. Biogeogr., 25, 479–500, https://doi.org/10.1046/j.1365-2699.1998.2530479.x, 1998.

Dupont, L. M.: Orbital scale vegetation change in Africa, Quaternary Sci. Rev., 30, 3589–3602, https://doi.org/10.1016/j.quascirev.2011.09.019, 2011.

Dupont, L. M. and Hooghiemstra, H.: The Saharan-Sahelian boundary during the Brunhes chron, Acta Bot. Neerl., 38, 405–415, https://doi.org/10.1111/j.1438-8677.1989.tb01372.x, 1989.

Dupont, L. M. and Kuhlmann, H.: Glacial-interglacial vegetation change in the Zambezi catchment, Quaternary Sci. Rev., 155, 127–135, https://doi.org/10.1016/j.quascirev.2016.11.019, 2017.

Dupont, L. M., Beug, H.-J., Stalling, H., and Tiedemann, R.: First palynological results from ODP Site 658 at 21° N west off Africa: pollen as climate indicators, edited by: Ruddiman, W. F., Sarnthein, M., Baldauf, J., and Shipboard Scientists, Proc. ODP Sci. Results, 108, College Station TX (Ocean Drilling Program), 93–111, 1989.

Dupont, L. M., Caley, T., Kim, J.-H., Castañeda, I., Malaizé, B., and Giraudeau, J.: Glacial-interglacial vegetation dynamics in South Eastern Africa coupled to sea surface temperature variations in the Western Indian Ocean, Clim. Past, 7, 1209–1224, https://doi.org/10.5194/cp-7-1209-2011, 2011a.

Dupont, L. M., Caley, T., Kim, J.-H., Castañeda, I. S., Malaizé, B., and Giraudeau, J.: Pollen distribution of sediment core MD96-2048 from the Western Indian Ocean, https://doi.org/10.1594/PANGAEA.771285, PANGAEA, 2011b.

Dupont, L. M., Caley, T., and Castañeda, I. S.: Pollen and Spores of sediment core MD96-2048 Pleistocene, https://doi.org/10.1594/PANGAEA.897922, PANGEA, 2019

Ehleringer, J. R., Cerling, T. E., and Helliker, B. R.: C$_4$ photosynthesis, atmospheric CO$_2$, and climate, Oecologia, 112, 285–299, https://doi.org/10.1007/s004420050311, 1997.

Foley, J., Kutzbach, J. E., Coe, M. T., and Levis, S.: Feedbacks between climate and boreal forests during the Holocene epoch, Nature, 371, 52–54, https://doi.org/10.1038/371052a0, 1994.

Ganopolski, A. and Calov, R.: The role of orbital forcing, carbon dioxide and regolith in 100 kyr glacial cycles, Clim. Past, 7, 1415–1425, https://doi.org/10.5194/cp-7-1415-2011, 2011.

Gasse, F. and Van Campo, E.: Late Quaternary environmental changes from a pollen and diatom record in the southern tropics (Lake Tritrivakely, Madagascar), Palaeogeogr. Palaeocl., 167, 287–308, https://doi.org/10.1016/S0031-0182(00)00242-X, 2001.

Hammer, Ø., Harper, D. A. T., and Ryan, P. D.: PAST: Paleontological Statistics Software Package for Education and Data Analysis, Palaeontol. Electron., 4, 1–9, 2001.

Ivory, S. J. and Russell, J.: Climate, herbivory, and fire controls on tropical African forest for the last 60 ka, Quaternary Sci. Rev., 148, 101–114, https://doi.org/10.1016/j.quascirev.2016.07.015, 2016.

Ivory, S. J., Lézine, A.-M., Vincens, A., and Cohen, A. S.: Waxing and waning of forests: Late Quaternary biogeography of southeast Africa, Glob. Change Biol., 2018, 1–13, https://doi.org/10.1111/gcb.14150, 2018.

Izumi, K. and Lézine, A.-M.: Pollen-based biome reconstructions over the past 18 000 years and atmospheric CO$_2$ impacts on vegetation in equatorial mountains of Africa, Quaternary Sci. Rev., 152, 93–103, https://doi.org/10.1016/j.quascirev.2016.09.023, 2016.

Jansen, J. H. F., Kuijpers, A., and Troelstra, S. R.: A mid-Brunhes climatic event: long-term changes in global atmosphere and ocean circulation, Science, 232, 619–622, https://doi.org/10.1126/science.232.4750.619, 1986.

Johnson, T. C., Brown, E. T., Mcmanus, J., Barry, S., Barker, P., and Gasse, F.: A high-resolution paleoclimate record spanning the past 25 000 years in southern East Africa, Science, 296, 113–132, https://doi.org/10.1126/science.1070057, 2002.

Johnson, T. C., Werne, J. P., Brown, E. T., Abbott, A., Berke, M., Steinman, B. A., Halbur, J., Conteras, S., Grosshuesch, S., Deino, A., Lyons, R. P., Scholz, C. A., Schouten, S., and Sinninghe Damsté, J. S.: A progressively wetter climate in southern East Africa over the past 1.3 million years, Nature, 537, 220–224, https://doi.org/10.1038/nature19065, 2016.

Jolly, D. and Haxeltine, A.: Effect of low glacial atmospheric CO$_2$ on tropical African montane vegetation, Science, 276, 786–788, https://doi.org/10.1126/science.276.5313.786, 1997.

Jury, M. R., Valentine, H. R., and Lutjeharms, J. R.: Influence of the Agulhas Current on summer rainfall along the southeast coast of South Africa, J. Appl. Meteorol., 32, 1282–1287, https://doi.org/10.1175/1520-0450(1993)032<1282:IOTACO>2.0.CO;2, 1993.

Kersberg, H.: Beiheft zu Afrika-Kartenwerk Serie S: Südafrika (Moçambique, Swaziland, Republik Südafrika), Bl. 7, Vegetationsgeographie, Gebrüder Borntraeger, Berlin, Germany, 182 pp., 1996.

Köhler, E. and Brückner, P.: De Pollenmorphologie der afrikanischen *Buxus*- und *Notobuxus*-Arten (Buxaceae) und ihre systemstische Bedeutung, Grana, 21, 71–82, https://doi.org/10.1080/00173138209427683, 1982.

Köhler, E. and Brückner, P.: The genus *Buxus* (Buxaceae): aspects of its differentiation in space and time, Plant Syst. Evol., 162, 267–283, https://doi.org/10.1007/978-3-7091-3972-1_14, 1989.

Kotze, D. and O'Connor, T. G.: Vegetation variation within and among palustrine wetlands along an altitudinal gradient in KwaZulu-Natal, South Africa, Plant Ecol., 146, 77–96, https://doi.org/10.1023/A:1009812300843, 2000.

Lisiecki, L. E. and Raymo, M. E.: A Pliocene-Pleistocene stack of 57 globally distributed benthic $\delta^{18}O$ records, Paleoceanography, 20, 1–17, https://doi.org/10.1029/2004PA001071, 2005.

Lüthi, D., Le Floch, M., Bereiter, B., Blunier, T., Barnola, J.-M., Siegenthaler, U., Raynaud, D., Jouzel, J., Fischer, H., Kawamura, K., and Stocker, T. F.: High-resolution carbon dioxide concentration record 650 000–800 000 years before present, Nature, 453, 379–382, https://doi.org/10.1038/nature06949, 2008.

Lyu, A., Lu, H., Zeng, L., Zhang, H., Zhang, E., and Yi, S.: Vegetation variation of loess deposits in the southeastern Inner Mongolia, NE China over the past ∼ 1.08 million years, J. Asian Earth Sci., 155, 174–179, https://doi.org/10.1016/j.jseaes.2017.11.013, 2018.

Maher Jr., L. J.: Nomograms for computing 0.95 confidence limits of pollen data, Rev. Palaeobot. Palyno., 13, 85–93, https://doi.org/10.1016/0034-6667(72)90038-3, 1972.

Maher Jr., L. J.: Statistics for microfossil concentration measurements employing samples spiked with marker grains, Rev. Palaeobot. Palyno., 32, 153–191, https://doi.org/10.1016/0034-6667(81)90002-6, 1981.

Marchant, R., Taylor, D., and Hamilton, A: Late Pleistocene and Holocene history at Mubwindi Swamp, Southwest Uganda, Quaternary Res., 47, 316–328, https://doi.org/10.1006/qres.1997.1887, 1997.

Martin, A. K.: The influence of the Agulhas Current on the physiographic development of the northernmost Natal Valley (S.W. Indian Ocean), Mar. Geol., 39, 259–276, https://doi.org/10.1016/0025-3227(81)90075-X, 1981.

Miller, S. M. and Gosling, W. D.: Quaternary forest associations in lowland tropical West Africa, Quaternary Sci. Rev., 84, 7–25, https://doi.org/10.1016/j.quascirev.2013.10.027, 2014.

Mucina, L. and Rutherford, M. C.: The vegetation of South Africa, Lesotho and Swaziland.: Strelitzia, 19. South African National Biodiversity Institute, Pretoria, South Africa, 807 pp., 2006.

Mudelsee, M. and Stattegger, K.: Exploring the structure of the mid-Pleistocene revolution with advanced methods of time-series analysis, Geol. Rundsch., 86, 499–511, https://doi.org/10.1007/s005310050157, 1997.

Owen, R. B., Muiruri, V. M., Lowenstein, T. K., Renaut, R. W., Rabideaux, N., Luo, S., Deino, A. L., Sier, M. J., Dupont-Nivet, G., Mcnulty, E. P., Leet, K., Cohen, A., Campisano, C., Deocampo, D., Shen, C.-C., Billingsley, A., and Mbuthia, A.: Progressive aridification in East Africa over the last half million years and implications for human evolution, P. Natl. Acad. Sci. USA, 115, 11174–11179, https://doi.org/10.1073/pnas.1801357115, 2018.

Paillard, D.: The Plio-Pleistocene climatic evolution as a consequence of orbital forcing on the carbon cycle, Clim. Past, 13, 1259–1267, https://doi.org/10.5194/cp-13-1259-2017, 2017.

Past Interglacials Working Group Of Pages: Interglacials of the last 800 000 years, Rev. Geophys., 54, 162–219, https://doi.org/10.1002/2015RG000482, 2016.

Prentice, I. C. and Harrison, S. P.: Ecosystem effects of CO_2 concentration: evidence from past climates, Clim. Past, 5, 297–307, https://doi.org/10.5194/cp-5-297-2009, 2009.

Prentice, I. C., Cleator, S. F., Huang, Y. H., Harrison, S. P., and Roulstone, I.: Reconstructing ice-age palaeoclimates: Quantifying low-CO_2 effects on plants, Global Planet. Change, 149, 166–176, https://doi.org/10.1016/j.gloplacha.2016.12.012, 2017.

Reason, C. J. C. and Mulenga, H.: Relationships between South African rainfall and SST anomalies in the Southwest Indian Ocean, Int. J. Climatol., 19, 1651–1673, https://doi.org/10.1002/(SICI)1097-0088(199912)19:15<1651::AID-JOC439>3.0.CO;2-U, 1999.

Sage, J. P.: The evolution of C_4 Photosynthesis, New Phytol., 161, 341–370, https://doi.org/10.1111/j.1469-8137.2004.00974.x, 2004.

Schefuß, E., Kuhlmann, H., Mollenhauer, G., Prange, M., and Pätzold, J.: Forcing of wet phases in southeast Africa over the past 17 000 years, Nature, 480, 509–512, https://doi.org/10.1038/nature10685, 2011.

Scholz, C. A., Cohen, A. S., and Johson, T. C.: Southern hemisphere tropical climate over the past 145 ka: Results of the Lake Malawi Scientific Drilling Project, East Africa (preface to special issue): Palaeogeogr. Palaeocl., 303, 1–2, https://doi.org/10.1016/j.palaeo.2011.01.001, 2011.

Schüler, L. and Hemp, A.: Atlas of pollen and spores and their parent taxa of Mt Kilimanjaro and tropical East Africa, Quatern. Int., 425, 301–386, https://doi.org/10.1016/j.quaint.2016.07.038, 2016.

Scott, L.: Late Quaternary fossil pollen grains from the Transvaal, South Africa, Rev. Palaeobot. Palynol., 36, 241–278, https://doi.org/10.1016/0034-6667(82)90022-7, 1982.

Scott, L.: Vegetation history and climate in the Savanna biome South Africa since 190 000 ka: a comparison of pollen data from the Tswaing Crater (the Pretoria Saltpan) and Wonderkrater, Quatern. Int., 57–58, 215–223, https://doi.org/10.1016/S1040-6182(98)00062-7, 1999.

Scott, L.: Grassland development under glacial and interglacial conditions in southern Africa: review of pollen, phytolith and isotope evidence, Palaeogeogr. Palaeocl., 177, 47–57, https://doi.org/10.1016/S0031-0182(01)00351-0, 2002.

Scott, L. and Thackeray, J. F.: Multivariate analysis of late Pleistocene and Holocene pollen spectra from Wonderkrater, Transvaal, South Africa: S. Afr. J. Sci., 83, 93–98, 1987.

Simon, M. H., Ziegler, M., Bosmans, J., Barker, S., Reason, C. J. C., and Hall, I. R.: Eastern South African hydrocli-

mate over the past 270 000 years, Sci. Rep.-UK, 5, 1–10, https://doi.org/10.1038/srep18153, 2015.

Singarayer, J. S. and Burrough, S. L.: Interhemispheric dynamics of the African rainbelt during the late Quaternary, Quaternary Sci. Rev., 124, 48–67, https://doi.org/10.1016/j.quascirev.2015.06.021, 2015.

Stock, W. D., Chuba, D. K., and Verboom, G. A.: Distribution of South African C_3 and C_4 species of Cyperaceae in relation to climate and phylogeny, Austral Ecol., 29, 313–319, https://doi.org/10.1111/j.1442-9993.2004.01368.x, 2004.

Sun, Y., An, Z., Clemens, S. C., Bloemendal, J., and Vandenberghe, J.: Seven million years of wind and precipitation variability on the Chinese Loess Plateau, Earth Planet. Sc. Lett., 297, 525–535, https://doi.org/10.1016/j.epsl.2010.07.004, 2010.

Swann, A. L., Fung, I. Y., Levis, S., Bonan, G. B., and Doney, S. C.: Changes in Arctic vegetation amplify high-latitude warming through the greenhouse effect, P. Natl. Acad. Sci. USA, 107, 1295–1300, https://doi.org/10.1073/pnas.0913846107, 2010.

Torres, V., Hooghiemstra, H., Lourens, L., and Tzedakis, P. C.: Astronomical tuning of long pollen records reveals the dynamic history of montane biomes and lake levels in the tropical high Andes during the Quaternary, Quaternary Sci. Rev., 63, 59–72, https://doi.org/10.1016/j.quascirev.2012.11.004, 2013.

Tyson, P. D. and Preston-Whyte, R. A.: The weather and climate of Southern Africa, Oxford University Press, Cape Town, South Africa, 396 pp., 2000.

Tzedakis, P. C., Hooghiemstra, H., and Pälike, H.: The last 1.35 million years at Tenaghi Philippon: revised chronostratigraphy and long-term vegetation trends, Quaternary Sci. Rev., 25, 3416–3430, https://doi.org/10.1016/j.quascirev.2006.09.002, 2006.

Tzedakis, P. C., Raynaud, D., Mcmanus, J. F., Berger, A., Brovkin, V., and Kiefer, T.: Interglacial diversity, Nat. Geosci., 2, 753–755, https://doi.org/10.1038/ngeo660, 2009.

Vincens, A., Lézine, A.-M., Buchet, G., Lewden, D., Le Thomas, A., and Contributors: African pollen database inventory of tree and shrub pollen types, Rev. Palaeobot. Palyno., 145, 135–141, https://doi.org/10.1016/j.revpalbo.2006.09.004, 2007.

Weltje, G. J.: End-member modeling of compositional data: numerical-statistical algorithms for solving the explicit mixing problem, Math. Geol., 29, 503–549, https://doi.org/10.1007/BF02775085, 1997.

White, F.: The vegetation of Africa, Natural Rescourses Research, 20. UNESCO, Paris, France, 356 pp., 3maps, 1983.

Wu, H., Guiot, J., Brewer, S., and Guo, Z.: Climatic changes in Eurasia and Africa at the last glacial maximum and mid-Holocene: reconstruction from pollen data using inverse vegetation modelling, Clim. Dynam., 29, 211–229, https://doi.org/10.1007/s00382-007-0231-3, 2007.

Yin, Q. Z.: Insolation-induced mid-Brunhes transition in Southern Ocean ventilation and deep-ocean temperature, Nature, 494, 222–225, https://doi.org/10.1038/nature11790, 2013.

Yin, Q. Z. and Berger, A.: Insolation and CO_2 contribution to the interglacial climate before and after the Mid-Brunhes Event, Nat. Geosci., 3, 243–246, https://doi.org/10.1038/ngeo771, 2010.

Yin, Q. Z. and Berger, A.: Individual contribution of insolation and CO_2 to the interglacial climates of the past 800,000 years, Clim. Dynam., 38, 709–724, https://doi.org/10.1007/s00382-011-1013-5, 2012.